Electronic Supplementary Material (ESI) for Physical Chemistry Chemical Physics.
This journal is © the Owner Societies 2019

SUPPORTING INFORMATION

Combined co-solvent and pressure effect on kinetics of a peptide hydrolysis: An activity-based approach

Received 00th January 20xx,
Accepted 00th January 20xx

DOI: 10.1039/x0xx00000x

Michael Knierbein[#a], Anton Wangler[#a], Trung Quan Luong[b], Roland Winter[b], Christoph Held*[a] and Gabriele Sadowski[a]

Materials

All Chemicals used in this work, their supplier and purity are given in Table S1.

Table S1. Chemicals used in this work including purity and supplier.

Component	Purity	Supplier
α-Chymotrypsin	>85%	Sigma Aldrich
N-Succinyl-L-phenylalanine-*p*-nitroanilide	>98%	Sigma Aldrich
urea	>99.5%	Acros Organics
Trimethylamine *N*-oxide	>98%	TCI
Dimethyl sulfoxide	>99.9>%	Sigma Aldrich

Estimation of α-CT pure-component PC-SAFT parameters

Two of the PC-SAFT pure-component parameters (m_i^{seg}, σ_i) and the association sites N_i^{assoc} of the enzyme α-CT were determined based on the amino acids sequence of the enzyme according to [ref SI 1]. The primary structure of α-CT is given in Figure S1.

```
        10         20         30         40         50
CGVPAIQPVL SGLSRIVNGE EAVPGSWPWQ VSLQDKTGFH FCGGSLINEN
        60         70         80         90        100
WVVTAAHCGV TTSDVVVAGE FDQGSSSEKI QKLKIAKVFK NSKYNSLTIN
       110        120        130        140        150
NDITLLKLST AASFSQTVSA VCLPSASDDF AAGTTCVTTG WGLTRYTNAN
       160        170        180        190        200
TPDRLQQASL PLLSNTNCKK YWGTKIKDAM ICAGASGVSS CMGDSGGPLV
       210        220        230        240
CKKNGAWTLV GIVSWGSSTC STSTPGVYAR VTALVNWVQQ TLAAN
```

Figure S1. Amino acid sequence (primary structure) of the enzyme α-chymotrypsin (α-CT) in single-letter amino acid code.

PC-SAFT pure-component parameters m_i^{seg}, σ_i and the association sites N_i^{assoc}(Hydrogen bond donor: Hydrogen bond acceptor) were determined based on the PC-SAFT parameters of the single amino acids from literature [ref SI 2]. The resulting parameters are given in Table S2.

Table S2. Determined PC-SAFT pure-component parameters segment number m_i^{seg}, segment diameter σ_i and association scheme N_i^{assoc} (hydrogen bond donor:hydrogen bond acceptor) of α-CT according to the amino acid sequence (primary structure) given in Figure S1.

Single Letter	Amino acid	number	m_i^{seg}	σ_i[Å]	HB acceptor	HB donor
G	glycine	23	4.849	2.327	0	0
A	alanine	22	5.464	2.522	0	0
L	leucine	19	8.303	2.7	0	0
M	methionine	2	16.025	2.149	1	0
F	phenylalanine*	6	5.464	2.522	0	0
W	tryptophan[#]	8	7.023	2.284	1	0
K	lysine	14	11.672	2.377	1	0
Q	glutamine[+]	10	3.024	3.478	1	0
E	glutamic acid	5	3.024	3.478	0	1
S	serine	28	7.023	2.284	0	0
P	proline	9	6.981	2.548	0	0
V	valine	23	7.485	2.588	0	0
I	isoleucine°	10	8.303	2.7	0	0
C	cysteine	10	7.739	2.384	1	0
Y	tyrosine	4	8.139	2.279	0	0
H	histidine	2	6.071	2.852	0	1
R	arginine	4	9.908	2.657	2	0
N	asparagine	14	2.999	3.366	1	0
D	aspartic acid	9	2.999	3.366	0	1
T	threonine	23	6.329	2.605	0	0
	∑	245	1610.324	2.627	67	17

* Parameters inherited from alanine
\# Parameters inherited from serine
\+ Parameters inherited from glutamic acid
° Parameters inherited from leucine

According to previous works on biomolecules, we only used data of aqueous solutions to fit parameters. The dispersion-energy parameter u_i/k_B, the association-energy parameter $\epsilon^{A_iB_i}/k_B$ and the association-volume parameter $\kappa^{A_iB_i}$ were afterwards fitted to one $B22$ data point (Table S5) and to density data of α-CT/buffer systems which were free of co-solvent. The result of this parameter fit is presented in Figure S2 for aqueous densities. We decided not to use ternary data for parameter fitting of the enzyme, according to our previous work on biomolecules [SI-ref 2].

---

[a] Laboratory of Thermodynamics, TU Dortmund University, Emil-Figge-Str. 70, 44227 Dortmund, Germany.
[b] Physical Chemistry I, TU Dortmund University, Otto-Hahn-Str. 4a, 44227 Dortmund, Germany.
shared first authors.
* E-mail: christoph.held@tu-dortmund.de

The ternary data of α-CT, co-solvent and water was only used to determine the binary interaction parameter between enzyme and co- solvent.

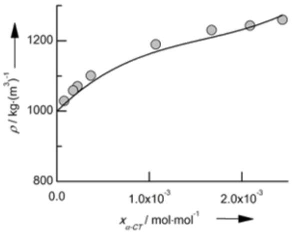

Figure S2. Densities ρ of aqueous solutions of α-CT at 25°C, 1 bar and pH 8. Symbols: Experimental data, Table S3. Line: PC-SAFT.

Table S3. Experimental densities of α-CT+ water at 25°C, 1 bar and pH 8.

Mole fraction α-CT	Density [kg m^{-3}]
7.93E-05	1028.44
1.76E-04	1058.54
2.24E-04	1070.58
3.69E-04	1100.62
1.07E-03	1189.68
1.67E-03	1230.13
2.09E-03	1243.10
2.44E-03	1259.78

A list of all pure-component parameters used in this work is given in Table S4.

Table S4. Overview of the PC-SAFT pure-component parameters used for activity coefficient predictions in this work.

Component	m_i^{seg}	σ_i [Å]	$\frac{u_i}{k_B}$ [K]	N_i^{assoc}	$\frac{\epsilon^{A_iB_i}}{k_B}$ [K]	$\kappa^{A_iB_i}$ [-]
water [ref SI 3]	1.204	[A]	353.95	1:1	2425.7	0.0451
SPNA [ref SI 4]	6.744	3.48	340.15	1:1	3219.1	0.0098
urea [ref SI 5]	4.242	2.45	368.23	1:1	3068.7	0.0010
DMSO [ref SI 6]	2.922	3.28	355.69	1:1	0	0.0451
TMAO [ref SI 7]	8.928	2.25	245.44	1:1	0	0.0451
α-CT [B]	1610.324	2.63	348.74	67:17	5713.8	1.0

[A] $\sigma_i = 2.7927 + 10.11 \cdot \exp(-0.01775 \cdot T) - 1.417 \cdot \exp(0.01146 \cdot T)$, [B] This work

Determination of binary-interaction parameters between α-CT / solvent and α-CT /co-solvent

The binary interaction parameters k_{ij} (shown in Equation (9)) between α-CT and the respective solvent/co-solvent were fitted to osmotic coefficients ϕ of α-CT solutions in the presence of the respective co-solvent. Osmotic coefficients of α-CT were obtained through the measurement of the second osmotic virial coefficient B_{22} by static light scattering. For a detailed description of the measurements of B_{22}, the reader is referred to previous work, e.g. [ref SI 8]. B_{22} was used to estimate ϕ in water based on Equation (1) and in the presence of an additional co-solvent based on Equation (2).

$$\phi = 1 + B_{22} \cdot m_{\alpha-CT} \left[\frac{mol}{kg_{water}}\right] \qquad (1)$$

$$\phi = 1 + B_{22} \cdot m_{\alpha-CT} \left[\frac{mol}{kg_{water}}\right] + \left(\phi^{ref} - 1\right) \qquad (2)$$

In Equation (2) a correction term is required. As ϕ for a binary mixture of water-co-solvent has to be accounted for, ϕ^{ref} is introduced. ϕ^{ref} is the osmotic coefficient of the water-co-solvent (enzyme free) solution that can be modeled with PC-SAFT or taken from literature data [ref SI 7]. B_{22} values determined in this work for α-CT in buffer and under the influence of the co-solvents DMSO and TMAO is listed in Table S5.

Table S5. Determined second osmotic virial coefficients B_{22} of α-CT in water (neat) and under the influence of the co-solvents DMSO, TMAO and urea at 25 °C, 1 bar and pH 8.

Co-solvent	$m_{co-solvent} \left[\frac{mol}{kg_{water}}\right]$	$B_{22} \left[\frac{kg_{water}}{mol}\right]$
neat	-	-615.75
DMSO	2.1	-481.25
TMAO	0.5	-226.10
urea	1	-156.25

A list of all binary interaction parameters used in this work is given in Table S6.

Table S6. Overview of the PC-SAFT binary interaction parameters used for activity coefficient predictions in this work.

Binary system	k_{ij} [-]
water-SPNA[A]	-0.132
water-urea[A]	-0.044
water-DMSO[A]	-0.065
water-TMAO[A]	-0.075
water-α-CT[B]	-0.067
α-CT-urea[B]	-0.35
α-CT-DMSO[B]	-0.6
α-C-TMAO[B]	-0.03

[A] ref SI 4 [B] This work

Thermodynamic model PC-SAFT

The activity coefficients of all reacting agents were calculated based on the pure-component reference state indicated by the subscript $0i$, while the activity coefficient of the enzyme was calculated based on the hypothetical ideal 1 molal aqueous solution reference state indicate by the superscript $*$. The activity coefficients were calculated with the respective fugacity coefficients φ_i based on the residual chemical potential μ_i^{res}, the Boltzmann constant k_B, the temperature T, the number density ρ and the residual Helmholtz energy a^{res} as shown in Equations (3) to (6).

$$\gamma_i = \frac{\varphi_i}{\varphi_{0i}} \qquad (3)$$

$$\gamma_i^* = \frac{\varphi_i}{\varphi_i^\infty} \qquad (4)$$

$$ln(\varphi_i) = \frac{\mu_i^{res}}{k_B \cdot T} - ln\left(1 + \left(\frac{\partial\left(\frac{a^{res}}{k_B \cdot T}\right)}{\partial \rho}\right)_{T,V}\right) \qquad (5)$$

$$\begin{aligned}\frac{\mu_i^{res}}{k_B \cdot T} = \frac{a^{res}}{k_B \cdot T} &+ Z - 1 \\ &+ \left(\frac{\partial\left(\frac{a^{res}}{k_B \cdot T}\right)}{\partial x_i}\right)_{T,V,x_{k\neq i}} \\ &- \sum_{j=1}^{N}\left(\frac{\partial\left(\frac{a^{res}}{k_B \cdot T}\right)}{\partial x_j}\right)_{T,V,x_{k\neq j}}\end{aligned} \qquad (6)$$

In Equation (6) Z denotes to the compressibility factor and x_i to the mole fraction of the component *i*. The residual Helmholtz energy a^{res}, which is required for calculations of μ_i^{res} and φ_i, was predicted with the PC-SAFT equation of state.

$$a^{res} = a^{hc} + a^{disp} + a^{assoc} \qquad (7)$$

This work accounts for four contributions in the prediction of a^{res}, which are a^{hc} (hard-chain forces), a^{disp} (dispersion interactions) and a^{assoc} (hydrogen bonding). PC-SAFT uses five pure-component parameters for the description of uncharged components capable of forming hydrogen bonds: The segment number m_i^{seg}, the segment diameter σ_i, the dispersion-energy parameter u_i/k_B, the association-energy parameter $\epsilon^{A_iB_i}/k_B$ and the association-volume parameter $\kappa^{A_iB_i}$. Pure-component parameters of water, SPNA, TMAO, DMSO and urea were taken from literature. The parameter fit for the enzyme α-CT has been presented in the beginning of the SI.

For the prediction of mixture properties, proposed combining rules of Berthelot and Lorenz (Equation (8) and (9)) and Wolbach-Sandler (Equation (10) and (11)) have been applied to the calculation of the mean segment diameter, mean dispersion-energy parameter and mean association-energy parameter in this work. Note that only one binary-interaction parameter k_{ij} was used in this work, as shown in Equation (9).

$$\sigma_{ij} = \frac{1}{2} \cdot (\sigma_i + \sigma_j) \qquad (8)$$

$$u_{ij} = \sqrt{u_i \cdot u_j} \cdot (1 - k_{ij}) \qquad (9)$$

$$\epsilon^{A_iB_j} = \frac{1}{2} \cdot (\epsilon^{A_iB_i} + \epsilon^{A_jB_j}) \qquad (10)$$

$$\kappa^{A_iB_j} = \sqrt{\kappa^{A_iB_i} \cdot \kappa^{A_jB_j}} \cdot \left(\frac{\sqrt{\sigma_i \cdot \sigma_j}}{\sigma_{ij}}\right)^3 \qquad (11)$$

The parameter fit performed to obtain the required PC-SAFT parameters is based on a Levenberg-Marquardt algorithm (damped least squares method), which was used to minimize the objective function OF given in Equation (12), in which y^{mod} and y^{exp} denote modeled and experimental values.

$$OF = \sum_{m=1}^{y_m} \sum_{k=1}^{NP_{y_m}} \left(1 - \left(\frac{y_m^{mod}}{y_m^{exp}}\right)_k\right)^2 \qquad (12)$$

Overview of experimental and predicted K_M and k_{cat} values

An overview of all measured and predicted values of K_M and k_{cat} values in this work is given in Table S7.

Table S7. Overview over the measured and predicted kinetic constants under combined co-solvent and pressure influence.

$p\ [bar]$	*Co-solvent m = mol/kg$_{water}$*	$K_M^{obs}\ \left[\frac{mmol}{kg_{water}}\right]$	$K_M^{pre}\ \left[\frac{mmol}{kg_{water}}\right]$	$k_{cat}^{obs}\ \left[\frac{1}{s}\right]$	$k_{cat}^{pre}\ \left[\frac{1}{s}\right]$
1	neat	1.76 ± 0.12	-	0.023 ± 0.002	-
	0.5 m TMAO	1.93 ± 0.18	2.00	0.026 ± 0.002	0.023
	1 m urea	2.50 ± 0.20	2.41	0.018 ± 0.001	0.019
	2.1 m DMSO	2.58 ± 0.56	3.74	0.019 ± 0.003	0.017
	4.2 m DMSO	6.21 ± 0.99	5.78	0.018 ± 0.003	0.015
500	neat	1.67 ± 0.07	1.62	0.026 ± 0.001	0.027
	0.5 m TMAO	1.76 ± 0.07	1.72	0.027 ± 0.001	0.026
	1 m urea	2.33 ± 0.10	2.09	0.021 ± 0.001	0.022
	2.1 m DMSO	2.49 ± 0.12	3.56	0.020 ± 0.001	0.020
	4.2 m DMSO	6.09 ± 0.74	5.65	0.019 ± 0.003	0.017
1000	neat	1.48 ± 0.04	1.48	0.030 ± 0.001	0.031
	0.5 m TMAO	1.57 ± 0.05	1.55	0.030 ± 0.001	0.030
	1 m urea	2.08 ± 0.10	1.86	0.024 ± 0.001	0.025
	2.1 m DMSO	2.27 ± 0.20	3.38	0.022 ± 0.001	0.023
	4.2 m DMSO	6.23 ± 0.58	6.01	0.021 ± 0.002	0.019
1500	neat	1.35 ± 0.04	-	0.035 ± 0.001	-
	0.5 m TMAO	1.44 ± 0.04	1.39	0.035 ± 0.001	0.035
	1 m urea	1.81 ± 0.06	1.57	0.028 ± 0.001	0.028
	2.1 m DMSO	2.45 ± 0.14	3.65	0.027 ± 0.001	0.026
	4.2 m DMSO	6.17 ± 0.20	5.92	0.023 ± 0.001	0.022
2000	neat	1.20 ± 0.09	1.24	0.042 ± 0.002	0.041
	0.5 m TMAO	1.29 ± 0.06	1.26	0.039 ± 0.002	0.040
	1 m urea	1.63 ± 0.006	1.42	0.034 ± 0.001	0.032
	2.1 m DMSO	2.37 ± 0.17	3.62	0.031 ± 0.002	0.030
	4.2 m DMSO	5.94 ± 0.52	5.79	0.025 ± 0.002	0.025

Determination and prediction of K_M^a and k_{cat}^a

In a first step K_M^a and k_{cat}^a were determined for 1 bar and 1500 bar under neat (co-solvent free) conditions at 20 °C and pH 8. This was done based on the experimentally determined K_M^{obs} and k_{cat}^{obs} values. The Lineweaver-Burk plot required for the determination of the kinetic constants is given in Figure S3.

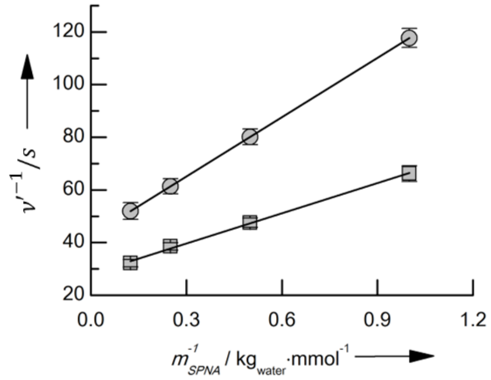

Figure S3. Lineweaver-Burk plot used to determine K_M^{obs} and k_{cat}^{obs} for the hydrolysis of SPNA catalyzed by α-CT at 20 °C and pH 8. The reciprocal reaction rate ν'^{-1} is plotted over the reciprocal initial molality of SPNA m_{SPNA}^{-1} for 1 bar (circles) and 1500 bar (squares). Lines represent the fit lines used for the linearization.

The resulting K_M^{obs} and k_{cat}^{obs} values are listed in Table S8.

Table S8. Overview of the experimentally determined K_M^{obs} and k_{cat}^{obs} values for the hydrolysis of SPNA catalysed by α-CT at 20 °C, pH 8 and the pressure 1 bar and 1500 bar.

$p\ [bar]$	$K_M^{obs}\ \left[\frac{mmol}{kg_{water}}\right]$	$k_{cat}^{obs}\ \left[\frac{1}{s}\right]$
1	1.76 ± 0.12	0.023 ± 0.001
1500	1.35 ± 0.04	0.035 ± 0.001

In a next step a linear correlation of K_M^{obs} and k_{cat}^{obs} over the pressure p according to Equations 5 and 6 in the main text were used to determine K_M^{pre} and k_{cat}^{pre} for the pressures 500, 1000 and 2000 bar. The respective plots of $\ln\left(K_M^{obs}\right)$ and $\ln\left(k_{cat}^{obs}\right)$ over p are given in Figure S4.

The predicted values of K_M^{pre} and k_{cat}^{pre} are listed in Table S9.

Table S9. Overview of the predicted values of K_M^{pre} and k_{cat}^{pre} for hydrolysis of SPNA catalyzed by α-CT at 20 °C and pH 8. Predictions are listed for the pressure of 500 bar, 1000 bar and 2000 bar based on Equations 5 and 6 in the main text and Figure S4.

$p\ [bar]$	$K_M^{pre}\ \left[\frac{mmol}{kg_{water}}\right]$	$k_{cat}^{pre}\ \left[\frac{1}{s}\right]$
500	1.61	0.027
1000	1.48	0.031
2000	1.24	0.041

To determine the respective activity-based kinetic constants K_M^a and k_{cat}^a, activity coefficients of the substrate SPNA γ_{SPNA} at $m_{SPNA} = K_M$ and the activity coefficient of the enzyme $\gamma^*_{\alpha-CT}$ at $m_{SPNA} = 0.96 \cdot m_{SPNA}(\nu = k_{cat})$ were determined with PC-SAFT based on the parameters listed in Table S4 and Table S6. An overview of the determined activity coefficients and the respective activity-based kinetic constants for the pressures p = 1 bar, 500 bar, 1000 bar, 1500 bar and 2000 bar is given in Table S10.

Note, that γ_{SPNA} refers to the reference state “pure component”, while $\gamma^*_{\alpha-CT}$ denotes the reference state “1 molal hypothetically ideal solution”. For more information the reader is referred to [ref SI 9].

Table S10. Overview about the predicted activity coefficients γ_{SPNA} for $m_{SPNA} = K_M$ and $\gamma^*_{\alpha-CT}$ for $m_{SPNA} = 0.96 \cdot m_{SPNA}(\nu = k_{cat})$ for the measured values of K_M and k_{cat} indicated by the superscript *obs* and the predicted values indicated by the superscript *pre*. Additionally, the resulting activity-based constants K_M^a and k_{cat}^a are listed for the pressures 1 bar, 500 bar, 1000 bar, 1500 bar and 2000 bar.

$p\ [bar]$	K_M^{obs} $\left[\frac{mmol}{kg_{water}}\right]$	γ_{SPNA} $\left[\frac{kg_{water}}{mmol}\right]$	$K_M^a\ [-]$	$k_{cat}^{obs}\ \left[\frac{1}{s}\right]$	$\gamma^*_{\alpha-CT}\ [-]$	$k_{cat}^a\ \left[\frac{1}{s}\right]$
1	1.76 ± 0.12	0.0013	0.0023	0.023 ± 0.001	0.965	0.022
1500	1.35 ± 0.04	0.0017	0.0023	0.035 ± 0.001	0.938	0.032

$p\ [bar]$	K_M^{pre} $\left[\frac{mmol}{kg_{water}}\right]$	γ_{SPNA} $\left[\frac{kg_{water}}{mmol}\right]$	$K_M^a\ [-]$	$k_{cat}^{pre}\ \left[\frac{1}{s}\right]$	$\gamma^*_{\alpha-CT}\ [-]$	$k_{cat}^a\ \left[\frac{1}{s}\right]$
500	1.61	0.0011	0.0019	0.027	0.954	0.026
1000	1.48	0.0013	0.0019	0.031	0.946	0.029
2000	1.24	0.0025	0.0030	0.041	0.930	0.038

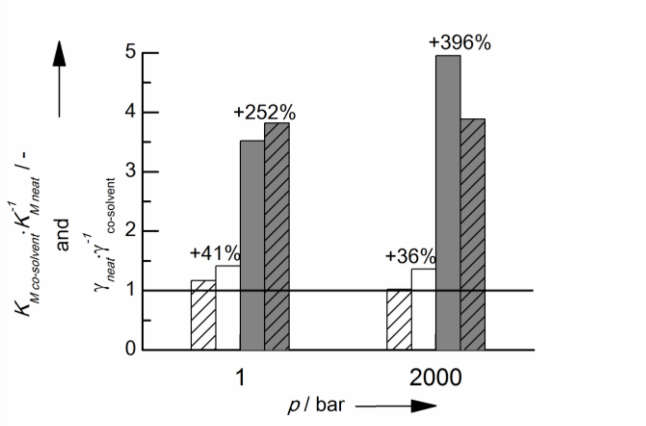

Figure S4. Observed Michaelis constant of the co-solvent reaction system rationalized to the observed Michaelis constant of the neat reaction system and the activity coefficient of the neat system rationalized to the activity coefficient of the co-solvent system (shaded bars) for 1 mol/kg$_{water}$ urea (white bars) and 4.2 mol/kg$_{water}$ DMSO (grey bars) at 1 bar and at 2000 bar. The solid line at y=1 represents the ratio for the neat system.

It was observed that pressure may strengthen or weaken co-solvent effects. For a better illustration of pressure induced changes in the co-solvents’ effects on reaction kinetics a plot of the observed kinetic constants of the co-solvent reaction system rationalized to the observed kinetic constants of the neat reaction system is shown in Figure S4 and Figure S5. Further, the activity coefficient of the neat system rationalized to the activity coefficient of the co-solvent system is also added to these figures.

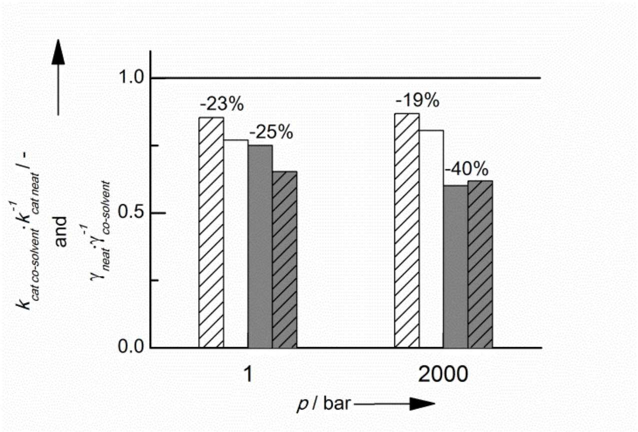

Figure S5. Observed catalytic constant of the co-solvent reaction system rationalized to the observed catalytic constant of the neat reaction system and the activity coefficient of the neat system rationalized to the activity coefficient of the co-solvent system (shaded bars) for 1 mol/kg$_{water}$ urea (white bars) and 4.2 mol/kg$_{water}$ DMSO (grey bars) at 1 bar and at 2000 bar. The solid line at y=1 represents the ratio for the neat system.

The results show that co-solvent effects of urea are decreased at high-pressure condition compared to the neat system from 41 % to 36 % with respect to the Michaelis constant as well as from -23 % to -19 % with respect to the catalytic constant. Further, the PC-SAFT predictions by means of the activity coefficient agree well with these findings.

Pressure effects on the 4.2 mol/kg$_{water}$ DMSO systems show a contrary behaviour. Pressure strengthens the co-solvent effect of DMSO on reaction kinetics. This is shown by a deviation of the Michaelis constant compared to the neat system increasing from 252 % at 1 bar to 396 % at 2000 bar. Also, the effect of DMSO on the catalytic constant is strengthened by pressure from -25 % at 1 bar to -40% at 2000 bar.

Predicted primary plots

The predicted primary plots of the α-CT reaction under the influence of 0.5 mol/kg$_{water}$ TMAO and 1 mol/kg$_{water}$ urea are provided in Figure S6 and Figure S7.

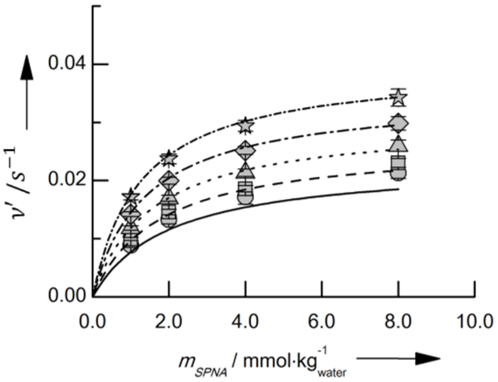

Figure S6. Primary plot of initial normalised reaction rate v' at 0.5 mol/kg$_{water}$ TMAO conditions plotted against the initial substrate molality m_{SPNA} at different pressures. Lines: PC-SAFT predictions, symbols: experimental data (circles: 1 bar, squares: 500 bar, triangles: 1000 bar, diamonds: 1500 bar, stars: 2000 bar).

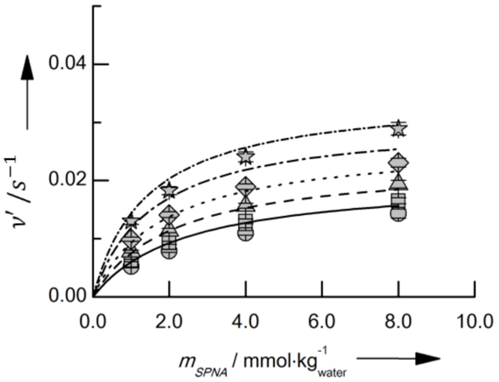

Figure S7. Primary plot of initial normalised reaction rate v' at 1 mol/kg$_{water}$ urea conditions plotted against the initial substrate molality m_{SPNA} at different pressures. Lines: PC-SAFT predictions, symbols: experimental data (circles: 1 bar, squares: 500 bar, triangles: 1000 bar, diamonds: 1500 bar, stars: 2000 bar).

References

SI ref 1: M. Hübner, C. Lodziak, H. T. J. Do and C. Held, *Fluid Phase Equilibria*, 2018, **472**, 62-74.
SI ref 2: C. Held, L. F. Cameretti and G. Sadowski, *Industrial & Engineering Chemistry Research*, 2011, **50**, 131-141.
SI ref 3: L. F. Cameretti and G. Sadowski, *Chemical Engineering and Processing: Process Intensification*, 2008, **47**, 1018-1025.
SI ref 4: A. Wangler, R. Canales, C. Held, T. Q. Luong, R. Winter, D. H. Zaitsau, S. P. Verevkin and G. Sadowski, *Physical chemistry chemical physics : PCCP*, 2018, **20**, 11317-11326.
SI ref 5: C. Held, T. Neuhaus and G. Sadowski, *Biophys Chem*, 2010, **152**, 28-39.
SI ref 6: M. Kleiner and J. Gross, *AIChE Journal*, 2006, **52**, 1951-1961.
SI ref 7: C. Held and G. Sadowski, *Fluid Phase Equilibria*, 2016, **407**, 224-235.
SI ref 8: M. Voges, M. Herhut, C. Held and C. Brandenbusch, *Fluid Phase Equilibria*, 2018, **465**, 65-72.
SI ref 9: C. Held and G. Sadowski, *Annual review of chemical and biomolecular engineering*, 2016, **7**, 395-414.